RESEARCH ARTICLE

Cerebral Microbleeds in Fragile X–Associated Tremor/Ataxia Syndrome

María Jimena Salcedo-Arellano, MD,[1,2,3,4] Jun Yi Wang, PhD,[2,5] Yingratana A. McLennan, BS,[1,2,3] Mai Doan, BS,[3,4] Ana Maria Cabal-Herrera, MD,[6] Sara Jimenez, BS,[3,4] Marisol W. Wolf-Ochoa, BS,[3,4] Desiree Sanchez, BS,[3,4] Pablo Juarez, BS,[3,4] Flora Tassone, PhD,[2,7] Blythe Durbin-Johnson, PhD,[8] Randi J. Hagerman, MD,[1,2] and Verónica Martínez-Cerdeño, PhD[2,3,4*]

[1]*Department of Pediatrics, University of California Davis School of Medicine, Sacramento, California, USA*
[2]*Medical Investigation of Neurodevelopmental Disorders (MIND) Institute, University of California Davis, Sacramento, California, USA*
[3]*Institute for Pediatric Regenerative Medicine and Shriners Hospitals for Children Northern California, Sacramento, California, USA*
[4]*Department of Pathology and Laboratory Medicine, UC Davis School of Medicine, Sacramento, California, USA*
[5]*Center for Mind and Brain, University of California Davis, Davis, California, USA*
[6]*Group on Congenital Malformations and Dysmorphology, Faculty of Health, Universidad del Valle (MACOS), Cali, Colombia*
[7]*Department of Biochemistry and Molecular Medicine, UC Davis School of Medicine, Sacramento, California, USA*
[8]*Division of Biostatistics, Department of Public Health Sciences, UC Davis School of Medicine, Sacramento, California, USA*

ABSTRACT: Background: Fragile X–associated tremor/ataxia syndrome is a neurodegenerative disease of late onset developed by carriers of the premutation in the fragile x mental retardation 1 (*FMR1*) gene. Pathological features of neurodegeneration in fragile X–associated tremor/ataxia syndrome include toxic levels of *FMR1* mRNA, ubiquitin-positive intranuclear inclusions, white matter disease, iron accumulation, and a proinflammatory state.
Objective: The objective of this study was to analyze the presence of cerebral microbleeds in the brains of patients with fragile X–associated tremor/ataxia syndrome and investigate plausible causes for cerebral microbleeds in fragile X–associated tremor/ataxia syndrome.
Methods: We collected cerebral and cerebellar tissue from 15 fragile X–associated tremor/ataxia syndrome cases and 15 control cases carrying *FMR1* normal alleles. We performed hematoxylin and eosin, Perls and Congo red stains, ubiquitin, and amyloid β protein immunostaining. We quantified the number of cerebral microbleeds, amount of iron, presence of amyloid β within the capillaries, and number of endothelial cells containing intranuclear inclusions. We evaluated the relationships between pathological findings using correlation analysis.
Results: We found intranuclear inclusions in the endothelial cells of capillaries and an increased number of cerebral microbleeds in the brains of those with fragile X–associated tremor/ataxia syndrome, both of which are indicators of cerebrovascular dysfunction. We also found a suggestive association between the amount of capillaries that contain amyloid β in the cerebral cortex and the rate of disease progression.
Conclusion: We propose microangiopathy as a pathologic feature of fragile X–associated tremor/ataxia syndrome. © 2021 International Parkinson and Movement Disorder Society

Key Words: FXTAS; *FMR1* premutation; neurodegeneration; cerebral microbleeds

***Correspondence to:** Verónica Martínez-Cerdeño, Shriners Hospitals for Children, 2425 Stockton Blvd., Sacramento CA 95817, USA; E-mail: vmartinezcerdeno@ucdavis.edu

Relevant conflicts of interest/financial disclosures: R.J.H. has received funding from Zynerba, Ovid, and the Azrieli Foundation for carrying out treatment studies in patients with fragile X syndrome (FXS). She has also consulted with Fulcrum, Ovid, and Zynerba regarding treatment studies in individuals with FXS. F.T. has received funds from Asuragen and Zynerba for studies in FXS and associated disorders. V.M.C. has consulted with Paxmedica, and received funding from Zynerba for organization of conferences in FXS and associated disorders.

Funding agencies: This research was supported by funds from the National Institute of Neurological Disorders and Stroke (NINDS) grant R01 1NS107131, the National Institute of Child Health and Human Development (NICHD) grant R01 HD036071, the MIND Institute Intellectual and Developmental Disabilities Research Center P50 HD103526, the National Center for Advancing Translational Sciences, National Institute of Health, through grant UL1 TR001860, and Shriners Hospitals for Children – Northern California.

Received: 9 February 2021; **Revised:** 18 February 2021; **Accepted:** 22 February 2021

Published online in Wiley Online Library (wileyonlinelibrary.com). DOI: 10.1002/mds.28559

Fragile X–Associated Tremor/Ataxia Syndrome

Fragile X–associated tremor/ataxia syndrome (FXTAS) was described 20 years ago in a series of cases of fragile x mental retardation 1 (*FMR1*) gene premutation male carriers (expansion between 55 and 200 CGG trinucleotide repeats) presenting with intention tremor and cerebellar ataxia.[1,2] The clinical presentation is variable, and as the disease progresses the patients experience worsening tremor, cerebellar ataxia, cognitive decline, peripheral neuropathy, and parkinsonism.[3,4] The age of clinical diagnosis is generally between 55 and 65 years old[5] and is more prevalent in males (~40%) than in females (~16%).[6,7] Females typically present with milder symptoms, less white matter (WM) hyperintensities (WMHs) on MRI, and slower progression.[8]

The neurotoxicity induced by the increased levels of *FMR1* mRNA is the main trigger of its pathogenesis.[9,10] Furthermore, the noncoding region of *FMR1* premutation mRNA has been proposed to be translated into multiple repeat associated non-AUG (RAN) peptides, including the FMRpolyG.[11] The neurotoxicity of this peptide lies in its ability to disrupt the structure of the neuronal nuclear lamina.[12] In addition, mitochondrial alterations and increased concentrations of intracellular calcium lead to an abnormal cellular response to DNA damage and increased neural vulnerability to reactive oxygen species.[13,14] The presence of ubiquitin-positive intranuclear inclusions in neurons and astrocytes[15,16] is the major pathologic criterion in the postmortem diagnosis of FXTAS.[17] These inclusions have also been reported in Purkinje cells[18] and in non-nervous tissues.[19] Other pathologic findings include WM disease (WMD)[16]; increased iron deposition in the putamen, the Purkinje layer of the cerebellum, and the choroid plexus[20-22]; and the presence of activated and senescent microglia.[23]

Cerebral Amyloid Angiopathy

We recently observed cerebral microbleeds (CMBs) in some cases of FXTAS during routine postmortem microscopic pathological examinations. Both cerebral amyloid angiopathy (CAA) and nonamyloid small vessel disease resulting from hypertension are known to underlie the appearance of CMBs. CAA-associated hemorrhages are superficial and because of the primary involvement of vessels in the cerebral cortex and meninges.[24] CAA type 1 affects capillaries, leptomeningeal and cortical arterioles, venules, small arteries, and veins; it is 4 times more likely than CAA type 2 to be associated with apolipoprotein E (*APOE) ε4*.[25] Patients with Alzheimer's disease (AD) and concomitant moderate to severe CAA are considered at higher risk for lobar intracerebral hemorrhages.[26,27] Dementia is suggested to occur in about 21%–50% of men with FXTAS, and the frequency increases in latter stages of the disease[5,6,28,29]; nevertheless, the prevalence of coexisting FXTAS and AD is unknown. A previous case–control study conducted in 2 primary dementia populations including AD did not find a difference in the frequency of *FMR1* premutation expansion between groups.[30] However, a postmortem case series in females with a definite diagnosis of FXTAS found that half of cases had concomitant AD pathology.[29] Similar neuropathological studies have not been conducted in males with FXTAS. In addition, the presence of at least 1 *APOE ε4* allele may contribute as a genetic factor predisposing to the development of FXTAS.[31] In the current study, we quantified the burden of CMBs and CAA and evaluated their relation in cases of FXTAS and controls.

Iron Deposition

The gradual deposit of iron in the process of aging is well known.[32-34] Increased levels of iron are present in the substantia nigra in Parkinson's disease[35,36] and in the putamen, caudate, and temporal gray matter (GM) in AD.[37-40] The motor and cognitive deficits found in patients with multiple sclerosis (MS) are correlated with excessive iron deposition in the GM.[41,42] Our prior studies reported mild iron accumulation in the Purkinje layer and the dentate nucleus of the cerebellum in a subset of FXTAS cases[21] and to a greater degree in the putamen and choroid plexus.[20,22] We quantified the area occupied by iron bound to hemosiderin and examined the association of iron deposits, if any, with the presence of CMBs.

Materials and Methods

Sample Collection

Tissue was obtained from 15 males with FXTAS and 15 age- and sex-matched control cases from the FXS/FXTAS brain repository at UC Davis (a node of the Hispanic-American Brain Bank for Neurodevelopmental Disorders – CENE). Specimens were obtained through consented autopsies with the approval of the institutional review board. FXTAS cases had symptoms for many years before death (mean ± SD, 8 ± 6.7 years) and were clinically diagnosed based on the presence of intention tremor, cerebellar ataxia, parkinsonism, memory, and executive function deficits and confirmed with the presence of *FMR1* premutation and postmortem ubiquitin-positive intranuclear inclusions in brain cells. Control tissue was obtained from subjects without any significant neurological history or the premutation. Age of FXTAS cases ranged from 58 to 85 years (average, 73.9 years). Control cases ranged in age from 53 to 81 years

(average, 68.8 years). The number of CGG repeats in the FXTAS group was between 67 and 119 repeats (additional data in Table 1).

Histology

Fixed samples from cerebral cortex Brodmann areas (BA)8, BA9, and BA24 and the cerebellum were immersed in 20% sucrose (Fisher Scientific, Fair Lawn, NJ) and embedded in optimal cutting temperature compound (Fisher Healthcare, Houston, TX). Blocks were cut on a freezing microtome at a 14-μm thickness.

CGG Sizing

Genomic DNA was isolated from brain tissue using standard procedures (Trizol reagent; Invitrogen, Carlsbad, CA). CGG repeat allele size was determined using PCR and Southern blot analysis.[43,44]

Cerebral Microbleeds Quantification

Although performing routine microscopic analysis of FXTAS brain samples, we observed that many cases presented with CMBs (Fig. 1). To assess if CMBs were a characteristic of FXTAS, we analyzed tissue from the cerebral cortex and cerebellum of 15 FXTAS cases and 15 control cases (Fig. 1). A blinded investigator evaluated the presence of CMBs in cerebral and cerebellar sections at 10× in hematoxylin and eosin (H&E)–stained tissue (yes/no) and classified the number of CMBs with the following scoring system: 0 = no CMBs; 1 = 1–2 small CMBs; 2 = 1 large or 3 small CMBs; 3 = ≥2 large or >3 small CMBs.

Perl's Staining

We treated sections in 1:1 10% potassium ferrocyanide (Fisher Scientific, Fair Lawn, NJ) and 20% hydrochloric acid (Fisher Scientific, Fair Lawn, NJ) for 10 minutes at room temperature, counterstained with Nuclear Fast red (Ricca Chemical, Arlington, TX), dehydrated with ethanol, cleared with xylene, and coverslipped with Permount (Fisher Scientific, Fair Lawn, NJ). Blue (Prussian blue) color confirmed the presence of iron bound to hemosiderin in ferric state.

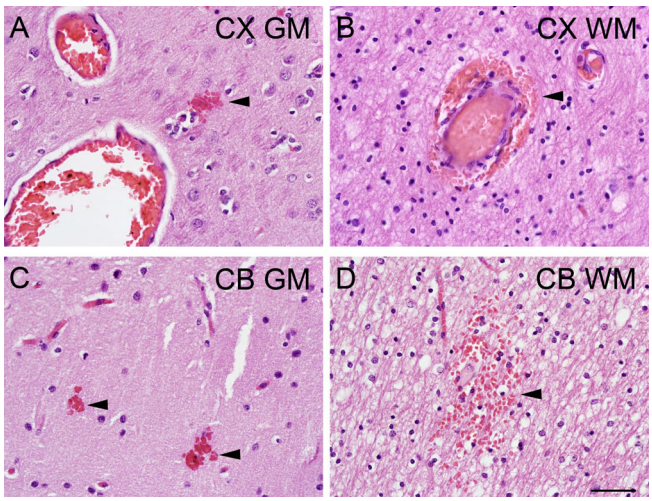

FIG. 1. Cerebral microbleeds (CMBs) stained with H&E. CMBs in WM and GM of (**A, B**) prefrontal cortex and (**C, D**) cerebellum. Scale bar: 50 μm. [Color figure can be viewed at wileyonlinelibrary.com]

TABLE 1. Subject characteristics by group

	Control (n = 15)	Case (n = 15)	All subjects (n = 30)	*P*
Age (years)				0.1008
n	15	15	30	
Mean (SD)	68.8 (8.8)	73.9 (7.9)	71.4 (8.6)	
Median (range)	68 (53–81)	75 (58–85)	71.5 (53–85)	
Anticoagulant medications				0.2926
None	3 (20%)	5 (33.3%)	8 (26.7%)	
Aspirin	1 (6.7%)	6 (40%)	7 (23.3%)	
Warfarin	2 (13.3%)	1 (6.7%)	3 (10%)	
Unknown	9 (60%)	3 (20%)	12 (40%)	
Stroke				0.0752
No	5 (33.3%)	13 (86.7%)	18 (60%)	
Yes	5 (33.3%)	2 (13.3%)	7 (23.3%)	
Unknown	5 (33.3%)	0	5 (16.7%)	
HTN				0.1760
No	1 (6.7%)	6 (40%)	7 (23.3%)	
Yes	8 (53.3%)	8 (53.3%)	16 (53.3%)	
Unknown	6 (40%)	1 (6.7%)	7 (23.3%)	

Subject characteristics in FXTAS and control cases. No subject characteristic differed significantly between FXTAS and control cases, although more control cases than FXTAS cases had a history of stroke.
P values for age are from a Wilcoxon rank sum test, and *P* values for categorical variables are from Fisher's exact test.

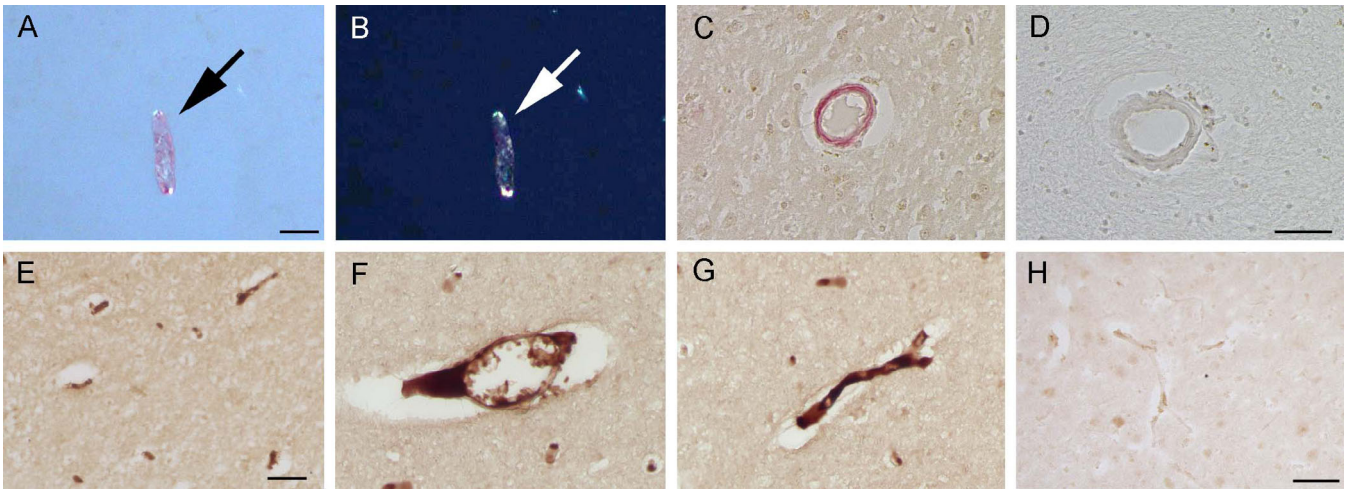

FIG. 2. Aβ in blood vessels. (**A, B**) Aβ in blood vessel in WM of the prefrontal cortex in FXTAS, stained with congo red under polarized light. (**C, D**) Aβ in blood vessels in WM of the prefrontal cortex, stained with congo red under bright-field. (**C**) Aβ blood vessels in WM of prefrontal cortex in FXTAS. (**D**) Negative Aβ blood vessels in WM in a control case. (**E-H**) Aβ blood vessels in prefrontal cortex stained with an antibody against Aβ. (**E-G**) Aβ blood vessels in prefrontal cortex WM in FXTAS. (**H**) Negative Aβ blood vessels in prefrontal cortex WM in a control case. Scale bar in A–B: 25 μm; C–D: 20 μm; E: 20 μm; F–H: 10 μm. [Color figure can be viewed at wileyonlinelibrary.com]

Congo Red Staining

We stained tissue with the modified Puchtler's Congo red amyloid method. We treated sections with modified Weigert's iron hematoxylin for 10 seconds, washed and placed in acid alcohol solution, followed by a filtered Congo red solution (C6767, Sigma-Aldrich, Saint Louis, MO) for 20 minutes, dehydrated in ethanol, cleared with xylene, and coverslipped with Permount (Fisher, Scientific, Fair Lawn, NJ).[45] Congo red–stained amyloid protein aggregates when in a compacted form.[46] Under cross-polarized light, stained aggregates show an apple-green birefringence[47] (Fig. 2).

Iron Quantification

We analyzed the area occupied by positive Prussian blue stain using NIH ImageJ software. Images from every FXTAS and control case were captured at 20× (Keyence microscope) and merged in a single image. We randomly selected areas of 5.04 mm^2/field from the cerebrum and 3.17 mm^2/field from the cerebellum and segmented the colors using the *colour deconvultion* plugin developed by G. Landini (http://www.dentistry.bham.ac.uk/landinig/software/cdeconv/cdeconv.html). We recorded the total percentage area occupied by Prussian blue for each sample.

Grading Systems for Cerebral Amyloid Angiopathy

We used 2 complementary grading systems to characterize CAA. The first, established by Olichney and colleagues in 1995,[48] classifies amyloid based on a 5-level positivity grading system, where 0 = no Aβ-positive blood vessels, 1 = scattered Aβ positivity, 2 = strong circumferential Aβ in some blood vessels, 3 = widespread strong, circumferential Aβ, and 4 = same as grade 3 with dysphoric changes. The second one, developed by Vonsattel el al,[49] grades CAA based on the degree of amyloid infiltration into the vessel wall, where mild = amyloid restricted to the tunica media, moderate = the tunica media is thicker than normal and replaced by amyloid, and severe = extensive deposition of amyloid, wall fragmentation, and leakage of blood through the vessel wall.

Ubiquitin and Amyloid Immunohistochemistry

We incubated sections in DIVA for 8 minutes at 110°C followed by 3% hydrogen peroxide, permeabilized and blocked in a Tris-buffered saline (TBS) solution containing Triton and donkey serum for 1 hour (75% TBS, 15% Triton, 10% serum), incubated with primary antibodies overnight at 4°C in a dark and humid box (rabbit antiubiquitin [1:150; Dako, Glostrup, Denmark] and polyclonal rabbit anti-β amyloid 1–42 [ab10148, 1:100; Abcam, Cambridge, UK]). On day 2, sections were incubated with donkey antirabbit biotinylated secondary antibody (1:150, Jackson ImmunoResearch, West Grove, PA) for 1 hour, incubated in Vectastain ABC kit (Vector Labs, Burlingame, CA) for 2 hours, developed in DAB kit (Vector Labs, Burlingame, CA), dehydrated with alcohols, cleared in xylene, and coverslipped.

Quantification of Ubiquitin-Positive Intranuclear Inclusions

For the visualization of ubiquitin-positive intranuclear inclusions in endothelial cells, 2 independent investigators quantified the first 20 capillaries encountered in the

cerebral and cerebellar WM and GM. We report the average of the 2 totals. We identified brain capillaries by their histological characteristics, a thin wall composed of continuous endothelial lining supported by a basement membrane and less than 8 μm in diameter, suitable for the passage of a single circulating blood cell.[50] Brain capillaries were characterized by the absence of astrocytic fibers, pericytes, and smooth muscle cells. We took images on an Olympus microscope using 20×–100× oil objectives.

Statistical Analysis

Statistical significance was defined as $P < 0.005$, per Benjamin and Berger,[51] with $P < 0.05$ considered suggestive. Age was compared between FXTAS and control cases using a Wilcoxon rank sum test, and categorical variables were compared between groups using Fisher's exact test. The associations between CMBs (which were ordered categorical variables) and group or clinical variables were analyzed using proportional odds logistic regression.[52] The relationships between inclusions and CMBs and between years to progression and CMBs were analyzed using linear regression. Years to disease progression was log-transformed prior to analysis to more closely satisfy model assumptions. Olichney scores were compared between groups and associated with clinical variables using proportional odds logistic regression. Vonsattel scores were compared between groups using Fisher's exact test and associated with clinical variables using logistic regression. Iron accumulation was compared between groups and associated with clinical variables using linear models. Iron percentage was log-transformed to more closely satisfy model assumptions. Analyses were conducted using R version 4.06.2 (2020-06-22).[53]

Results

Cerebral Microbleeds Are Common in FXTAS

All FXTAS brains had WM alterations in the cerebral and the cerebellar cortices, including WM vacuolization, axonal loss and widened perivascular spaces, consistent with the histological definition of WMD. We quantified the number of CMBs in the GM and WM of the prefrontal cerebral cortex and cerebellum of FXTAS and control cases (Fig. 1A–D).

We found that 56% of the FXTAS cases presented with CMBs in the WM of the cerebral and cerebellar cortices. The GM of the cerebral cortex was affected with CMBs in 40% of the cases, whereas 33% had CMBs in the GM of the cerebellum. In contrast, 6.6% of control cases had CMBs in cerebral WM, 20% in cerebral GM, and 6.6% in cerebellar GM and WM. FXTAS cases presented with a significant increase in the number of CMBs in the cerebral WM ($P = 0.000891$) and in the cerebellar WM ($P = 0.000822$) compared with control cases (Table 2). The difference in CMB scores in cerebellar GM (OR, 7.54; 95% CI, 1.01–156.27; $P = 0.0483$) suggested that FXTAS cases had higher odds of a greater number of CMBs than control cases. We did not find a significant difference in the cerebral GM. In addition, we did not find any association between a higher CMB score in the cerebral WM, cerebral GM, or cerebellar WM and age, number of CGG repeats, diagnosis of hypertension or stroke, use of anticoagulants or antiplatelets, and age at onset of FXTAS symptoms. However, data suggested that more years of disease progression might be associated with lower odds of a higher CMB score in the GM of the cerebellum ($P = 0.00657$). In other words, patients with FXTAS presenting with rapid disease progression had higher odds of a higher CMB score in the cerebellar GM (see supplementary material).

TABLE 2. Proportional odds logistic regression models of brain CMBs in cases and controls

	Odds ratio (95% confidence interval)	*P*
Cerebral cortex — WM	21.8 (3.13–451.19)	0.000891
Cerebral cortex — GM	2.82 (0.59–16.10)	0.197
Cerebellar cortex — WM	22.2 (3.19–458.70)	0.000822
Cerebellar cortex — GM	7.54 (1.01–156.27)	0.0483

Proportional odds logistic regression models comparing brain measures between FXTAS and control cases. FXTAS cases have significantly higher odds than control cases of worse CMB scores for cerebral cortex WM ($P = 0.000891$) and cerebellar cortex WM ($P = 0.000822$).
The odds ratio is the ratio of the odds of a worse versus better score for the brain measure in cases relative to controls.

Iron Accumulation in FXTAS

We visualized iron in the GM and WM of the prefrontal cerebral cortex and cerebellum using Perl's staining. There was no significant difference in iron occupancy between FXTAS and control cases across all the studied brain regions. There was no association between the area occupied by iron in the cerebral and cerebellar cortices of FXTAS cases and CGG repeats, age, rate of disease progression (in years), diagnosis of hypertension, stroke, and anticoagulant use.

Cerebral Amyloid Angiopathy in FXTAS

We quantified the amount of amyloid contained in blood vessels in sections from BA8, BA9, and cerebellar cortex stained with Congo red and Aβ immunohistochemistry (Fig. 2) in FXTAS and control cases. We found that FXTAS cases had higher odds of a higher CAA-Olichney score than control cases in the prefrontal cerebral cortex (OR, 4.44; 95% CI, 1.02–22.00; $P = 0.0466$). We did not find a difference in the

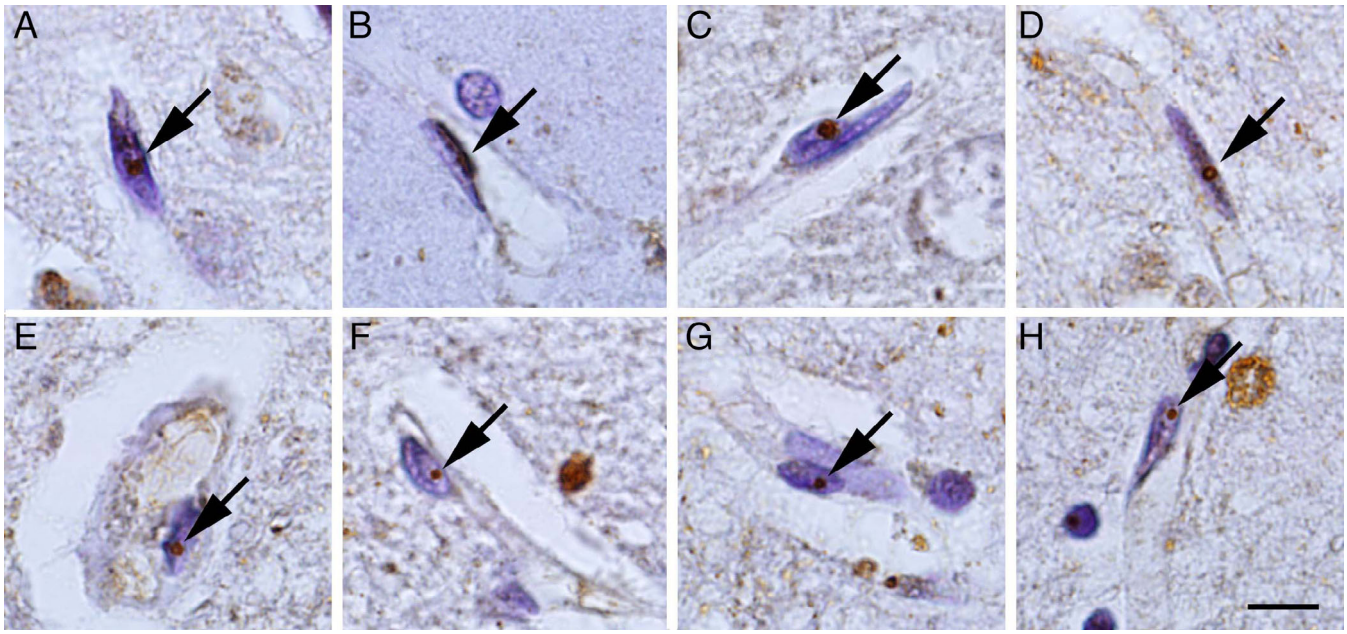

FIG. 3. Intranuclear inclusions in capillaries. (**A–H**) Ubiquitin-stained intranuclear inclusions (brown) in endothelial cells of capillaries in the prefrontal cortex of FXTAS cases. Endothelial cell nuclei are elongated and stained in purple with cresyl violet. Scale bar: 10 μm. [Color figure can be viewed at wileyonlinelibrary.com]

cerebellar cortex. Data suggest that a later onset of symptoms (P = 0.0457) and a faster progression of FXTAS before death (P = 0.0199) are associated with higher odds of a higher CAA-Olichney score in the cerebral cortex. Within FXTAS cases, although 35% had a mild and 28% a moderate CAA-Vonsattel score, none had a severe score. In contrast, only mild CAA-Vonsattel scores were registered in 35% of the controls. The difference in CAA-Vonsattel score between groups was not statistically significant.

Intranuclear Inclusions in Cerebral Endothelial Cells

Endothelial cells stained with an antibody against ubiquitin and Nissl presented with a pale violet cytoplasm, a dark violet nucleus, and brown intranuclear inclusions (Fig. 3). In FXTAS, only some capillaries presented endothelial cells with inclusions, and only some endothelial cells contained an inclusion within a given capillary (mean ± SD, 13% ± 12%). The percentage of capillaries compromised by intranuclear inclusions in their endothelial cells showed high variability from case to case (from 0% to 35%), and each case also had variable presentation across different brain areas. Higher CMB scores in the cerebral prefrontal cortical WM (P = 0.00598) and GM (P = 0.0201) were suggestively associated with a higher percentage of capillaries with inclusions. No association was found in the cerebellar cortex.

Discussion

Cerebral Microbleeds Are Expressions of Cerebrovascular Dysfunction in FXTAS

CMBs are microscopic bleedings associated with microangiopathy. The presence of CMBs in healthy subjects displays age-related increase in prevalence, ranging from 6.5% in 45- to 50-year-old individuals to 35.7% in individuals aged 80 years.[54] CMBs have a high prevalence in neurodegenerative diseases[55,56] and chronic systemic hypertension.[57] We found that most CMBs in FXTAS contained intact erythrocytes, suggesting that these were acute and not chronic CMBs. CMBs in the cortex of the human brain have been associated with the severe accumulation of Aβ in the walls of leptomeningeal and cortical small vessels,[58] defined as CAA.[59,60] CAA is found in ∼50%–80% of patients with dementia[61,62] and up to 95% of patients with AD.[63,64] We found higher CAA scores in FXTAS relative to controls in the cerebral cortex but not in the cerebellum. This suggests that the presence of CAA in patients with FXTAS may contribute to a vascular component of pathology. However, we did not confirm a correlation between CAA-Olichney- or CAA-Vonsattel scoring systems and CMB scores in FXTAS. Based on our analysis we cannot conclude that a greater number of CMBs is associated with more severe CAA in the studied brain regions of FXTAS cases. Our data are consistent with an AD study reporting a CAA correlation with age and the severity of amyloid plaque deposition, whereas the correlation with microinfarcts was

not statistically significant.[60] Further studies are needed to examine additional causes of vascular pathology in FXTAS.

Iron Deposits Are Located in Specific Brain Regions in FXTAS

Abnormal iron accumulation can occur as part of the normal aging process and in neurodegenerative diseases such as MS, AD, and CAA.[65] Our previous work indicated that iron accumulated in the putamen, choroid plexus, and dentate nucleus of the cerebellum in FXTAS.[20-22] However, we did not find a generalized increase in the amount of iron deposits within the FXTAS cases in the cerebellar and prefrontal cerebral cortex.[21] These data also suggest that the CMBs we describe in FXTAS are mostly acute, because chronic CMBs are associated with the deposition of blood-breakdown products, in particular, iron bound to hemosiderin, within perivascular macrophages, rarely detected in the studied areas of our FXTAS cases.

Endothelial Cells Have Intranuclear Inclusions in FXTAS

We showed that endothelial cells in FXTAS present with intranuclear inclusions. We hypothesize that endothelial cells containing intranuclear inclusions in FXTAS are compromised, producing changes in the endothelial structure that may cause the discontinuation of the contact between cells. This is supported by the observation of widened perivascular spaces, which may be an indication of a compromised blood–brain barrier. This alteration could translate into the breakage of the capillaries and/or the dysfunction of tight junctions, leading to increased vascular permeability and leakage of erythrocytes. Another possibility is that vascular changes are because of an inflammatory process that results in endothelial failure and neurovascular unit dysfunction.[66,67] FXTAS presents with a generalized proinflammatory state evident by the presence of microglial activation and microglial senescence,[23] iron deposition,[20-22] oxidative stress,[68,69] and elevated cytokine levels.[70] Most likely, a combination of events above, in addition to coexisting CAA, is responsible for the capillary dysfunction that underpins the presence of CMBs in FXTAS.

Microangiopathy Is a Component of FXTAS

We consider FXTAS a neurodegenerative disease associated with microangiopathy of the brain. Microangiopathy refers to conditions with damaged capillaries and characterized by CMBs, WMHs on MRI, reduced WM integrity, axonal injury, neuronal apoptosis, demyelination, oligodendrocyte damage, enlarged perivascular spaces, and brain atrophy,[66,71,72] all presenting in FXTAS. In addition, cerebrovascular dysfunction is linked to dementia, psychiatric disorders, and gait abnormalities, also characteristics of FXTAS.[73,74] Although features of microangiopathy have been reported in previous studies,[75,76] the current study demonstrates for the first time the evidence for a microangiopathy component in FXTAS pathology.

Limitations

Our data on postmortem analysis show that CMBs are common in the brain cortical WM in FXTAS. We have to be conservative with our conclusions given the studied sample size and variance of the measures. Some of the findings that were not significant during our evaluation might be because of the study being underpowered. We should also note that our findings relate only to the studied areas: prefrontal and cerebellar cortices. Additional studies are required to evaluate the burden of CMBs in other areas of the brain, including subcortical areas.

Conclusions

We have demonstrated the presence of CMBs and intranuclear inclusions in endothelial cells in FXTAS. There is an increased number of CMBs in the cerebral and cerebellar cortical WM of FXTAS compared with control cases and a possible association between CMB scores and the percentage of capillaries with intranuclear inclusions in the endothelial cells of the cerebral cortex. There is also a positive association between the number of capillaries containing Aβ in the cerebral prefrontal cortex of FXTAS cases and the age at onset of symptoms and the rate of disease progression. We concluded that the underlying pathogenic mechanism of FXTAS compromises cerebral vasculature, leading to a series of complex pathological changes and endothelial abnormalities. We suggest that the presence of CMBs in the cortical WM should be considered part of the histopathologic manifestation of FXTAS.

Acknowledgments: The authors acknowledge the great contribution from the donors and their families to the field of neurodegenerative disorders, especially for understanding of the neuropathology of FXTAS.

References

1. Hagerman RJ, Leehey M, Heinrichs W, et al. Intention tremor, parkinsonism, and generalized brain atrophy in male carriers of fragile X. Neurology 2001;57(1):127–130.
2. Hagerman RJ, Hagerman P. Fragile X-associated tremor/ataxia syndrome - features, mechanisms and management. Nat Rev Neurol 2016;12(7):403–412.
3. Jacquemont S, Hagerman RJ, Leehey M, et al. Fragile X premutation tremor/ataxia syndrome: molecular, clinical, and neuroimaging correlates. Am J Hum Genet 2003;72(4):869–878.
4. Grigsby J, Brega AG, Jacquemont S, et al. Impairment in the cognitive functioning of men with fragile X-associated tremor/ataxia syndrome (FXTAS). J Neurol Sci 2006;248(1–2):227–233.

5. Bourgeois JA, Cogswell JB, Hessl D, et al. Cognitive, anxiety and mood disorders in the fragile X-associated tremor/ataxia syndrome. Gen Hosp Psychiatry 2007;29(4):349–356.
6. Jacquemont S, Hagerman RJ, Leehey MA, et al. Penetrance of the fragile X-associated tremor/ataxia syndrome in a premutation carrier population. JAMA 2004;291(4):460–469.
7. Rodriguez-Revenga L, Madrigal I, Pagonabarraga J, et al. Penetrance of FMR1 premutation associated pathologies in fragile X syndrome families. Eur J Hum Genet 2009;17(10):1359–1362.
8. Hagerman RJ, Leavitt BR, Farzin F, et al. Fragile-X-associated tremor/ataxia syndrome (FXTAS) in females with the FMR1 premutation. Am J Hum Genet 2004;74(5):1051–1056.
9. Tassone F, Hagerman RJ, Taylor AK, Gane LW, Godfrey TE, Hagerman PJ. Elevated levels of FMR1 mRNA in carrier males: a new mechanism of involvement in the fragile-X syndrome. Am J Hum Genet 2000;66(1):6–15.
10. Berman RF, Buijsen RA, Usdin K, et al. Mouse models of the fragile X premutation and fragile X-associated tremor/ataxia syndrome. J Neurodev Disord 2014;6(1):25.
11. Todd PK, Oh SY, Krans A, et al. CGG repeat-associated translation mediates neurodegeneration in fragile X tremor ataxia syndrome. Neuron 2013;78(3):440–455.
12. Sellier C, Buijsen RAM, He F, et al. Translation of expanded CGG repeats into FMRpolyG is pathogenic and may contribute to fragile X tremor ataxia syndrome. Neuron 2017;93(2):331–347.
13. Song G, Napoli E, Wong S, et al. Altered redox mitochondrial biology in the neurodegenerative disorder fragile X-tremor/ataxia syndrome: use of antioxidants in precision medicine. Mol Med 2016; 22:548–559.
14. Robin G, López JR, Espinal GM, Hulsizer S, Hagerman PJ, Pessah IN. Calcium dysregulation and Cdk5-ATM pathway involved in a mouse model of fragile X-associated tremor/ataxia syndrome. Hum Mol Genet 2017;26(14):2649–2666.
15. Greco CM, Hagerman RJ, Tassone F, et al. Neuronal intranuclear inclusions in a new cerebellar tremor/ataxia syndrome among fragile X carriers. Brain 2002;125(Pt 8):1760–1771.
16. Greco CM, Berman RF, Martin RM, et al. Neuropathology of fragile X-associated tremor/ataxia syndrome (FXTAS). Brain 2006;129 (Pt 1):243–255.
17. Ma L, Herren AW, Espinal G, et al. Composition of the Intranuclear inclusions of fragile X-associated tremor/ataxia syndrome. Acta Neuropathol Commun 2019;7(1):143.
18. Ariza J, Rogers H, Monterrubio A, Reyes-Miranda A, Hagerman PJ, Martinez-Cerdeno V. A majority of FXTAS cases present with Intranuclear inclusions within Purkinje cells. Cerebellum 2016;15(5):546–551.
19. Greco CM, Soontrapornchai K, Wirojanan J, Gould JE, Hagerman PJ, Hagerman RJ. Testicular and pituitary inclusion formation in fragile X associated tremor/ataxia syndrome. J Urol 2007; 177(4):1434–1437.
20. Ariza J, Rogers H, Hartvigsen A, et al. Iron accumulation and dysregulation in the putamen in fragile X-associated tremor/ataxia syndrome. Mov Disord 2017;32(4):585–591.
21. Rogers H, Ariza J, Monterrubio A, Hagerman P, Martinez-Cerdeno V. Cerebellar mild iron accumulation in a subset of FMR1 Premutation carriers with FXTAS. Cerebellum 2016;15(5):641–644.
22. Ariza J, Steward C, Rueckert F, et al. Dysregulated iron metabolism in the choroid plexus in fragile X-associated tremor/ataxia syndrome. Brain Res 2015;1598:88–96.
23. Martínez-Cerdeño V, Hong T, Amina S, et al. Microglial cell activation and senescence are characteristic of the pathology FXTAS. Mov Disord 2018;33(12):1887–1894.
24. Mehndiratta P, Manjila S, Ostergard T, et al. Cerebral amyloid angiopathy-associated intracerebral hemorrhage: pathology and management. Neurosurg Focus 2012;32(4):E7.
25. Thal DR, Ghebremedhin E, Rub U, Yamaguchi H, Del Tredici K, Braak H. Two types of sporadic cerebral amyloid angiopathy. J Neuropathol Exp Neurol 2002;61(3):282–293.
26. van Veluw SJ, Charidimou A, van der Kouwe AJ, et al. Microbleed and microinfarct detection in amyloid angiopathy: a high-resolution MRI-histopathology study. Brain 2016;139(Pt 12):3151–3162.
27. Grabowski TJ, Cho HS, Vonsattel JP, Rebeck GW, Greenberg SM. Novel amyloid precursor protein mutation in an Iowa family with dementia and severe cerebral amyloid angiopathy. Ann Neurol 2001;49(6):697–705.
28. Juncos JL, Lazarus JT, Graves-Allen E, et al. New clinical findings in the fragile X-associated tremor ataxia syndrome (FXTAS). Neurogenetics 2011;12(2):123–135.
29. Tassone F, Greco CM, Hunsaker MR, et al. Neuropathological, clinical and molecular pathology in female fragile X premutation carriers with and without FXTAS. Genes Brain Behav 2012;11(5): 577–585.
30. Hall DA, Bennett DA, Filley CM, et al. Fragile X gene expansions are not associated with dementia. Neurobiol Aging. 2014;35(11): 2637–2638.
31. Silva F, Rodriguez-Revenga L, Madrigal I, Alvarez-Mora MI, Oliva R, Mila M. High apolipoprotein E4 allele frequency in FXTAS patients. Genet Med 2013;15(8):639–642.
32. Drayer B, Burger P, Darwin R, Riederer S, Herfkens R, Johnson GA. MRI of brain iron. AJR Am J Roentgenol 1986;147 (1):103–110.
33. Hallgren B, Sourander P. The effect of age on the non-haemin iron in the human brain. J Neurochem 1958;3(1):41–51.
34. Thomas LO, Boyko OB, Anthony DC, Burger PC. MR detection of brain iron. AJNR Am J Neuroradiol 1993;14(5):1043–1048.
35. Berg D, Hochstrasser H. Iron metabolism in Parkinsonian syndromes. Mov Disord 2006;21(9):1299–1310.
36. Gorell JM, Ordidge RJ, Brown GG, Deniau JC, Buderer NM, Helpern JA. Increased iron-related MRI contrast in the substantia nigra in Parkinson's disease. Neurology 1995;45(6):1138–1143.
37. Bartzokis G, Sultzer D, Cummings J, et al. In vivo evaluation of brain iron in Alzheimer disease using magnetic resonance imaging. Arch Gen Psychiatry 2000;57(1):47–53.
38. Bartzokis G, Sultzer D, Mintz J, et al. In vivo evaluation of brain iron in Alzheimer's disease and normal subjects using MRI. Biol Psychiatry 1994;35(7):480–487.
39. House MJ, St Pierre TG, Kowdley KV, et al. Correlation of proton transverse relaxation rates (R2) with iron concentrations in postmortem brain tissue from Alzheimer's disease patients. Magn Reson Med 2007;57(1):172–180.
40. House MJ, St Pierre TG, Foster JK, Martins RN, Clarnette R. Quantitative MR imaging R2 relaxometry in elderly participants reporting memory loss. AJNR Am J Neuroradiol 2006;27(2):430–439.
41. Brass SD, Benedict RH, Weinstock-Guttman B, Munschauer F, Bakshi R. Cognitive impairment is associated with subcortical magnetic resonance imaging grey matter T2 hypointensity in multiple sclerosis. Mult Scler 2006;12(4):437–444.
42. Tjoa CW, Benedict RH, Weinstock-Guttman B, Fabiano AJ, Bakshi R. MRI T2 hypointensity of the dentate nucleus is related to ambulatory impairment in multiple sclerosis. J Neurol Sci 2005;234 (1–2):17–24.
43. Filipovic-Sadic S, Sah S, Chen L, et al. A novel FMR1 PCR method for the routine detection of low abundance expanded alleles and full mutations in fragile X syndrome. Clin Chem 2010;56(3): 399–408.
44. Tassone F, Pan R, Amiri K, Taylor AK, Hagerman PJ. A rapid polymerase chain reaction-based screening method for identification of all expanded alleles of the fragile X (FMR1) gene in newborn and high-risk populations. J Mol Diagn 2008;10(1):43–49.
45. Center UoRM; Pages. https://www.urmc.rochester.edu/urmc-labs/pathology/stainsmanual/index.html?MODIFIEDPUCHTLERCONGOREDAMYLOIDMETHOD12020.
46. Wilcock DM, Gordon MN, Morgan D. Quantification of cerebral amyloid angiopathy and parenchymal amyloid plaques with Congo red histochemical stain. Nat Protoc 2006;1(3):1591–1595.
47. Howie AJ, Brewer DB, Howell D, Jones AP. Physical basis of colors seen in Congo red-stained amyloid in polarized light. Lab Invest 2008;88(3):232–242.

48. Olichney JM, Hansen LA, Hofstetter CR, Grundman M, Katzman R, Thal LJ. Cerebral infarction in Alzheimer's disease is associated with severe amyloid angiopathy and hypertension. Arch Neurol 1995;52(7):702–708.
49. Vonsattel JP, Myers RH, Hedley-Whyte ET, Ropper AH, Bird ED, Richardson EP Jr. Cerebral amyloid angiopathy without and with cerebral hemorrhages: a comparative histological study. Ann Neurol 1991;30(5):637–649.
50. Practical Surgical Neuropathology: A Diagnotic Approach. 2nd ed. Philadelphia, PA: Elsevier; 2018.
51. Benjamin DJ, Berger JO. Three recommendations for improving the use of p-values. Am Stat 2019;73(sup. 1):186–191.
52. Agresti A. Categorical Data Analysis. 2nd ed. New York, NY: John Wiley & Sons, Inc; 2002.
53. Team RC. 2019. https://www.R-project.org/. Accessed November 11, 2019.
54. Poels MM, Vernooij MW, Ikram MA, et al. Prevalence and risk factors of cerebral microbleeds: an update of the Rotterdam scan study. Stroke 2010;41(10 Suppl):S103–S106.
55. Lesnik Oberstein SA, van den Boom R, van Buchem MA, et al. Cerebral microbleeds in CADASIL. Neurology 2001;57(6): 1066–1070.
56. Dichgans M, Holtmannspotter M, Herzog J, Peters N, Bergmann M, Yousry TA. Cerebral microbleeds in CADASIL: a gradient-echo magnetic resonance imaging and autopsy study. Stroke 2002;33(1):67–71.
57. Kidwell CS, Saver JL, Villablanca JP, et al. Magnetic resonance imaging detection of microbleeds before thrombolysis: an emerging application. Stroke 2002;33(1):95–98.
58. Thal DR. The pre-capillary segment of the blood-brain barrier and its relation to perivascular drainage in Alzheimer's disease and small vessel disease. ScientificWorldJournal 2009;9:557–563.
59. Soontornniyomkij V, Lynch MD, Mermash S, et al. Cerebral microinfarcts associated with severe cerebral beta-amyloid angiopathy. Brain Pathol 2010;20(2):459–467.
60. Kovari E, Herrmann FR, Hof PR, Bouras C. The relationship between cerebral amyloid angiopathy and cortical microinfarcts in brain ageing and Alzheimer's disease. Neuropathol Appl Neurobiol 2013;39(5):498–509.
61. Ellis RJ, Olichney JM, Thal LJ, et al. Cerebral amyloid angiopathy in the brains of patients with Alzheimer's disease: the CERAD experience, Part XV. Neurology 1996;46(6):1592–1596.
62. Pfeifer LA, White LR, Ross GW, Petrovitch H, Launer LJ. Cerebral amyloid angiopathy and cognitive function: the HAAS autopsy study. Neurology 2002;58(11):1629–1634.
63. Greenberg SM, Briggs ME, Hyman BT, et al. Apolipoprotein E epsilon 4 is associated with the presence and earlier onset of hemorrhage in cerebral amyloid angiopathy. Stroke 1996;27(8): 1333–1337.
64. Jellinger KA. Alzheimer disease and cerebrovascular pathology: an update. J Neural Transm (Vienna) 2002;109(5–6):813–836.
65. Amaral LLF, Gaddikeri S, Chapman PR, et al. Neurodegeneration with brain iron accumulation: Clinicoradiological approach to diagnosis. J Neuroimaging 2015;25(4):539–551.
66. Hakim AM. Small Vessel Disease. Front Neurol 2019;10:1020.
67. Shoamanesh A, Preis SR, Beiser AS, et al. Inflammatory biomarkers, cerebral microbleeds, and small vessel disease: Framingham heart study. Neurology 2015;84(8):825–832.
68. Ross-Inta C, Omanska-Klusek A, Wong S, et al. Evidence of mitochondrial dysfunction in fragile X-associated tremor/ataxia syndrome. Biochem J 2010;429(3):545–552.
69. Giulivi C, Napoli E, Tassone F, Halmai J, Hagerman R. Plasma metabolic profile delineates roles for neurodegeneration, pro-inflammatory damage and mitochondrial dysfunction in the FMR1 premutation. Biochem J 2016;473(21):3871–3888.
70. Dufour BD, Amina S, Martinez-Cerdeno V. FXTAS presents with upregulation of the cytokines IL12 and TNFalpha. Parkinsonism Relat Disord 2020;82:117–120.
71. Rosano C, Marsland AL, Gianaros PJ. Maintaining brain health by monitoring inflammatory processes: a mechanism to promote successful aging. Aging Dis 2012;3(1):16–33.
72. Rosano C, Watson N, Chang Y, et al. Aortic pulse wave velocity predicts focal white matter hyperintensities in a biracial cohort of older adults. Hypertension 2013;61(1):160–165.
73. Kim HJ, Kang SJ, Kim C, et al. The effects of small vessel disease and amyloid burden on neuropsychiatric symptoms: a study among patients with subcortical vascular cognitive impairments. Neurobiol Aging 2013;34(7):1913–1920.
74. Pinter D, Ritchie SJ, Doubal F, et al. Impact of small vessel disease in the brain on gait and balance. Sci Rep 2017;7:41637.
75. Apartis E, Blancher A, Meissner WG, et al. FXTAS: new insights and the need for revised diagnostic criteria. Neurology 2012;79(18): 1898–1907.
76. Brunberg JA, Jacquemont S, Hagerman RJ, et al. Fragile X premutation carriers: characteristic MR imaging findings of adult male patients with progressive cerebellar and cognitive dysfunction. AJNR Am J Neuroradiol 2002;23(10):1757–1766.

Supporting Data

Additional Supporting Information may be found in the online version of this article at the publisher's web-site.

Authors' Roles

M.J.S.A. — conception, organization, and execution of the research project (review of medical histories, staining, microscopic and image analysis); writing of the first draft of the manuscript.

J.Y.W. — conception of the research project; writing of the first draft of the manuscript.

Y.A.M. — execution of the research project (tissue preparation, staining, microscopic analysis and imaging); writing of the first draft of the manuscript.

M.D. — execution of the research project (tissue preparation, staining, microscopic analysis, and imaging).

A.M.C.H. — execution of the research project (statistical analysis); writing of the first draft of the manuscript.

S.J. — execution of the research project (tissue preparation, staining, and imaging).

M.W.W.O. — execution of the research project (tissue preparation and staining).

D.S. — execution of the research project (tissue preparation, staining, and imaging).

P.J. — execution of the research project (tissue preparation).

F.T. — execution of the research project (CGG sizing).

B.D.J. — execution of the research project (statistical analysis); writing of the first draft of the manuscript.

R.J.H. — conception and organization of the research project; review and critique of the manuscript.

V.M.C. — conception, organization, and execution of the research project; writing of the first draft of the manuscript; review and critique of the manuscript.